

Transforming an Optical Pick-up-Head into an Accelerometer With UltraHigh Sensitivity

Shao-Kang Hung*, *Member, IEEE*, Chiao-Hua Cheng, Ming-Li Chiang, and Jih-Wei Chieh

Abstract—This paper proposes an accelerometer based on a commercial optical pick-up-head (PUH). An optical PUH is used to be part of an accelerometer by transforming the astigmatic measuring mechanism, the suspending wires, and the objective lens as the displacement sensor, the spring, and the seismic mass, respectively. Instead of adding an extra mass-damper-spring subsystem into the system in previous works, in our design we utilize the four suspending metal wires and the objective lens in an optical PUH. Thus, no extra component is needed and the system is more compact and easy to implement. Experimental results demonstrate that this cost-effective accelerometer has excellent linearity, ultrahigh sensitivity of 114 V/g, and an operating frequency of 20 Hz.

Index Terms—Acceleration measurement, CD recording, dynamic response, optical position measurement, vibration measurement

I. INTRODUCTION

ACCELEROMETERS work as a motion sensor, which senses acceleration. The vibration level of a bridge, a building floor, a spindle shaft, and the intensity of an earthquake are all measured by accelerometers. Becoming indispensable in everyone's daily life, accelerometers can be applied in various fields. In 1998, U.S. government amended Federal Motor Vehicle Safety Standard 208 (FMVSS 208) to require cars to be equipped dual front airbags, which are triggered by accelerometers. Most countries outside North America also mandated similar standards and created a big market for accelerometers. Modern digital cameras embed accelerometers to achieve "anti-shake" function. During temporary satellite signal loss, an advanced global positioning system (GPS) can adopt auxiliary accelerometer's information

Manuscript received March 4, 2013; revised June 27, 2013; accepted August 2, 2013. Date of publication October 16, 2013; date of current version February 5, 2014. This work was supported by the National Science Council of Taiwan under Grants NSC 98-2221-E-009-010-MY3 and NSC 101-2221-E-009-017. The Associate Editor coordinating the review process was Dr. Wei Gao. (*Corresponding author: S.-K. Hung.*)

S.-K. Hung is with the Department of Mechanical Engineering, National Chiao Tung University, Hsinchu 300, Taiwan (e-mail: skhung@mail.nctu.edu.tw).

C.-H. Cheng is with the Department of Mechanical Engineering, National Chiao Tung University, Hsinchu 300, Taiwan (e-mail: sly_9414019@yahoo.com.tw).

M.-L. Chiang was with the National Taiwan University, Taipei 10617, Taiwan. He is now with the Department of Electrical Engineering, National Taiwan University, Taipei 10617, Taiwan (e-mail: minglichang@ntu.edu.tw).

J.-W. Chieh was with the Department of Mechanical Engineering, National Chiao Tung University, Hsinchu 300, Taiwan (e-mail: rhowitizer2001@yahoo.com.tw).

Color versions of one or more of the figures in this paper are available online at <http://ieeexplore.ieee.org>.

Digital Object Identifier 10.1109/TIM.2013.2282427

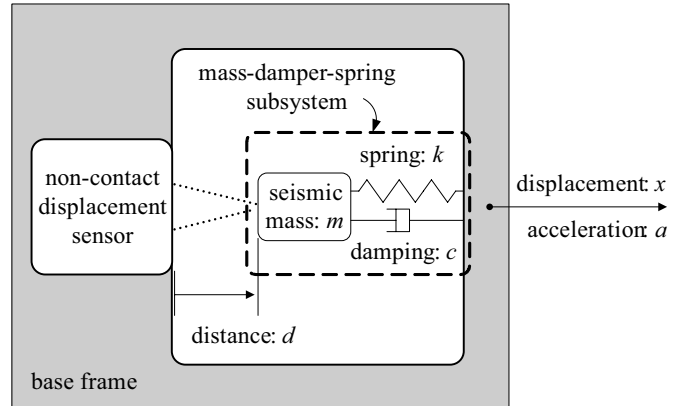


Fig. 1. Schematic structure of a typical accelerometer.

to navigate ceaselessly. Robots, especially humanoid ones, are installed accelerometers to stabilize complicated motions, such as walking, running, and even somersaulting. Accelerometers have also made revolution on video games. Nintendo Wii's controller has a 3-axis accelerometer (ADXL330, Analog Devices Inc.) inside and redefines the gaming experience completely. Via the motion sensing technology, people play video games in the physical world instead of the virtual world.

Referring to Fig. 1, a typical accelerometer consists of a base frame, a mass-damper-spring subsystem, and a non-contact displacement sensor to measure the distance d between the base frame and the seismic mass. The acceleration acting on the whole system is then derived from the measured displacement [1], and therefore the displacement sensor plays an important role.

A sensitive accelerometer must embed a sensitive displacement sensor inside. Published literatures discussed several displacement sensing mechanisms designed for accelerometers, including variable capacitive [2], resistive [3], piezoelectric [4], [5], piezoresistive [6], [7], electro-magnetic [8], and optical [9] categories. Among these methods, the digital-versatile-disk (DVD) pick-up-head (PUH) can be an ultrasensitive displacement sensor, which is suitable to make an accelerometer with a very good resolution. In our previous research [10], a DVD PUH-based displacement sensor has the resolution of $1.3 \text{ pmHz}^{-1/2}$ to detect the thermal vibration of a micro-cantilever with a bandwidth at 800 kHz. Since this DVD PUH has excellent performance, it was adopted in the developments of profilometers [11] and atomic force microscopes (AFMs) [12], which realized atomic resolution.

DVD PUH was utilized to develop 1-D [13] and 2-D accelerometers [14]–[16]. In these two systems, DVD PUH purely works as a displacement sensor and an extra mass-damper-spring subsystem is needed. However, any added device may make the whole system bulky (e.g., 94.5 g in the 1-D version) and limits its applicability. According to ISO 2954 standard, accelerometer’s weight should be less than one-tenth weight of the tested object. Additional mass-damper-spring subsystem also induces the drawback of slow dynamic response. In both 1-D and 2-D versions, the bandwidth is limited at 20% of the resonant frequency of the spring-mass subsystem. Relative to previous designs, our proposed accelerometer in this paper does not need to add extra mass-damper-spring subsystem and aforementioned drawbacks can be avoided. The implemented accelerometer has excellent linearity, ultrahigh sensitivity of 114 V/g, an operating frequency of 20 Hz for low frequency applications, and is cost-effective.

The remainder of this paper is organized as follows. After the principle of accelerometer and basics of DVD PUH are introduced in Section II, the details of instrument design are described and analyzed in Section III. The experimental results are reported in Section IV and the performance of the proposed accelerometer is summarized in the final section.

II. PRELIMINARY

A. Accelerometer Principle

The general structure of an accelerometer is shown in Fig. 1. The inertial force is equal to the elastic force when the system is accelerated to equilibrium and is shown as follows:

$$a = \frac{k}{m}x \quad (1)$$

where a is the acceleration, k is the spring constant, m is the seismic mass, and x is the relative displacement between the seismic mass and the base frame. If the resolution of x is given, the coefficient k/m determines the resolution of a . To achieve good resolution of a , the coefficient k/m should be small. In addition, the coefficient k/m is also the square of the undamped natural frequency of the mass-damper-spring system. Higher undamped natural frequency implies higher bandwidth of the accelerometer. In summary, it is a trade-off between good resolution and high bandwidth.

If the mass-damper-spring system has low damping, the magnitude of the acceleration can be correctly measured only when the acceleration acting on the base frame does not exceed 20% [13] of the resonant frequency of the mass-damper-spring system. On the contrary, adding proper damping helps to extend the bandwidth of the accelerometer. To design an accelerometer, the first parameter to be decided is the bandwidth. Note that the mass-damper-spring system to sense ultrasound (>20 kHz) is much different from the one to detect the movement of the Earth’s crust (0.1–10 Hz). Next, a displacement sensor with a matching bandwidth should be adopted. If the displacement sensor also has good resolution, linearity, and a suitable measuring range, an accelerometer with good performance can be accomplished.

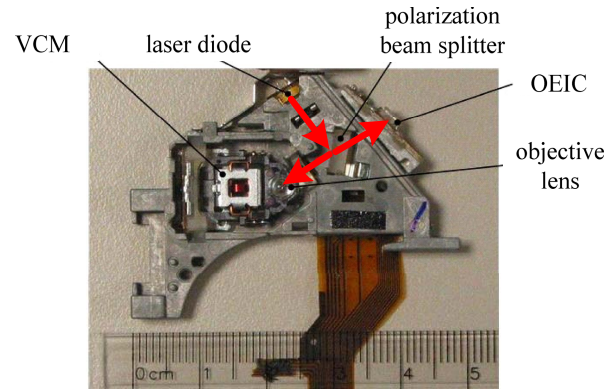


Fig. 2. Photograph of the DVD PUH used in this paper. The red arrows indicate the optical path. The total mass is 18 g.

TABLE I
SPECIFICATIONS OF THE DVD PUH

Laser	
wavelength	655 nm
typical power	0.23 W
operating current	82 mA
operating voltage	2.7 V
Objective lens	
numerical aperture	0.6
focal length	2.33 mm
working distance	1.28 mm

B. DVD PUH Basic

Fig. 2 illustrates the structure of a DVD PUH (Model: TOP 1100S, TopRay Technologies) used in this paper and the specifications of the selected DVD PUH are listed in Table I.

A typical DVD PUH consists of four parts: a laser diode as the light source, an opto-electric integrated circuit (OEIC) as the light sensor, an objective lens as the light condenser, and a voice coil motor (VCM) as an actuator to carry the objective lens. When a disk spins fast inside the DVD drive, it wobbles and the focusing condition becomes unstable. In order to maintain stable data reading or writing, VCM adjusts the position of the objective lens to track the motion of the disk’s surface via a feedback controller. The sensing mechanism of this feedback loop is introduced in the following.

As shown in Fig. 3, inside a DVD PUH, a laser beam emitted from a laser diode is first diffracted and collimated into three beams, and then focused onto an optical disk by an objective lens actuated by a VCM. The beams reflected from the disk are then directed back through the objective lens and, after passing through an astigmatic element, impinge onto the OEIC. The OEIC is composed of four split photosensors A–D, and four current preamplifiers for the four photosensors.

The detection of the laser beam focusing condition on the optical disk adopts the astigmatic measuring mechanism, which uses a cylindrical lens as a beam-shaping device [17]. When the laser beam is perfectly focused on the disk surface, the laser spot on the four central quadrant photosensors A to D is circular [see Fig. 4(b)], but when the disk surface is slightly higher or lower than the focus of the laser beam, the laser spot on the central quadrant sensors appears more elongated,

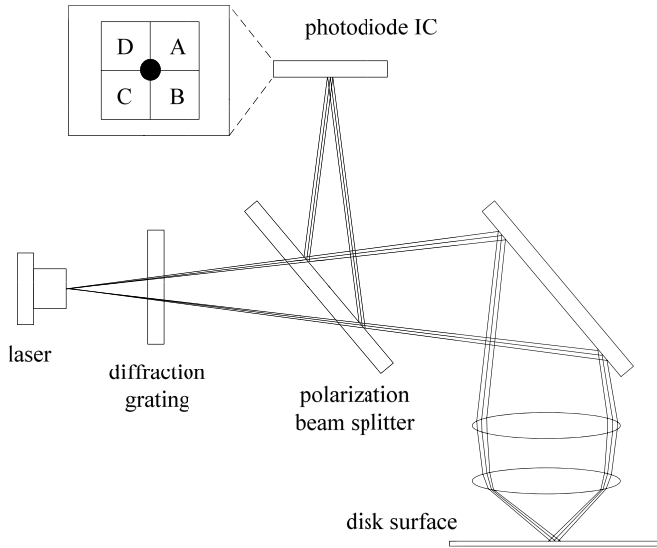


Fig. 3. Inside buildup and working principle of a typical DVD PUH.

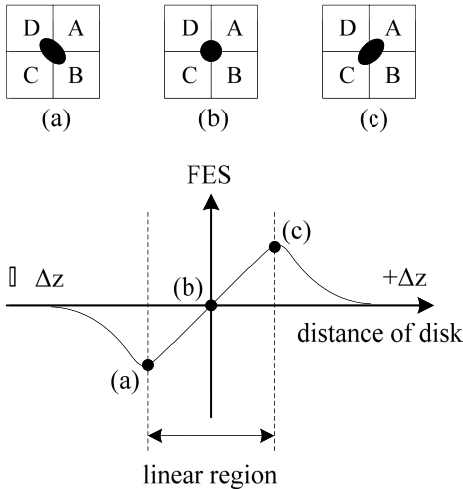


Fig. 4. Shape of laser spot and S-curve of FES. (a) Off focus, $FES < 0$. (b) On focus, $FES = 0$. (c) Off focus, $FES > 0$. (d) Linear region of FES.

as illustrated in Fig. 4(a) and (c). The shape change of the laser spot on the OEIC can be detected by the focus error signal (FES), which is defined as $(S_A + S_C) - (S_B + S_D)$, where S_A to S_D are the preamplifier output voltages of photo-sensors A to D. For a circular laser spot, FES is equal to zero. Fig. 4(d) shows the well-known S-curve for the relationship of the FES versus the vertical distance of the disk [18]. By experimentally measuring the FES, the VCM can drive the objective lens to focus the laser beam on the disk surface, or $FES = 0$.

As shown in Fig. 5, the four suspending metal wires of VCM support the objective lens. This kind of guiding system has several advantages, such as no friction, simple structure, and cost-effectiveness. These four metal wires act as the mechanical guidance as well as the electrical conductor. Utilizing the electromagnetic force, the position of the objective lens can be finely adjusted by applying appropriate voltage or current. Table II shows the specifications of the VCM.

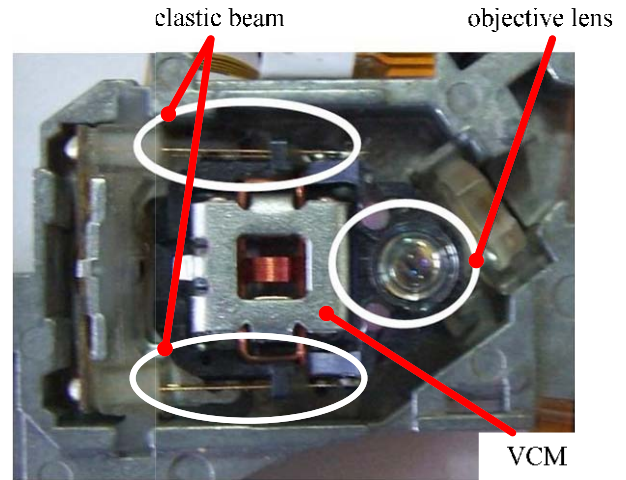


Fig. 5. Four elastic beams and objective lens build the spring-mass system in a PUH.

TABLE II
SPECIFICATIONS OF THE VCM

Focusing actuator	
working range	+1 mm/-0.55 mm or more
DC resistance of coil	4.5 Ω
Tracking actuator	
working range	± 0.4 mm or more
DC resistance of coil	4.2 Ω

In the DVD PUH application, the focusing condition may be unstable due to a wobbling disk. To always focus the laser on the data pits of the disk, the astigmatic sensing mechanism and the VCM play the roles of the sensor and the actuator in a feedback control system to maintain a constant gap between the disk and the objective lens.

If a DVD PUH is modified to be a displacement sensor, the objective lens should be glued firmly and the suspending metal wires should be cut off. In this paper, however, the objective lens is not fixed. To solve this problem, our study transforms the suspending wires and the objective lens into a mass-damper-spring system as described in Section III.

III. INSTRUMENT DESIGN

As stated previously, an accelerometer needs a displacement sensor and a mass-damper-spring system, which is usually made of an elastic cantilever beam with a block at the free end.

It is not new to modify a PUH to be a displacement sensor. In [13], the authors also use a DVD PUH as the displacement sensor in the accelerometer design. An extra elastic beam is added to connect the seismic mass and this mechanism is used to be the mass-damper-spring system. In our new design, the PUH can act as a displacement sensor and serves as a mass-damper-spring system at the same time. By regarding the four suspending metal wires and the objective lens in PUH as the mass-damper-spring system, it is not necessary to build an extra mass-damper-spring system as in [13] and thus the

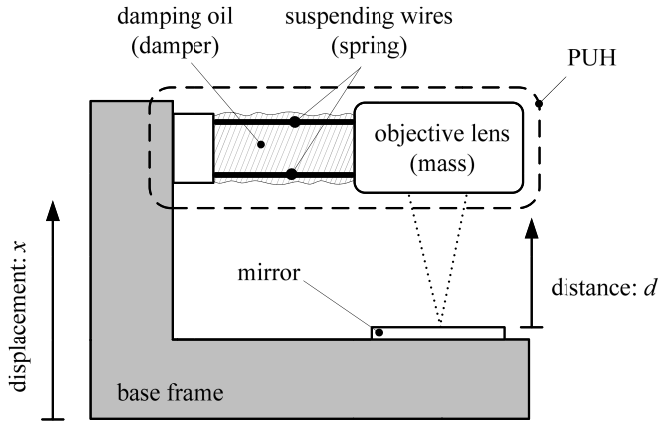


Fig. 6. Schematic illustration of the mechanical design of the proposed PUH accelerometer.

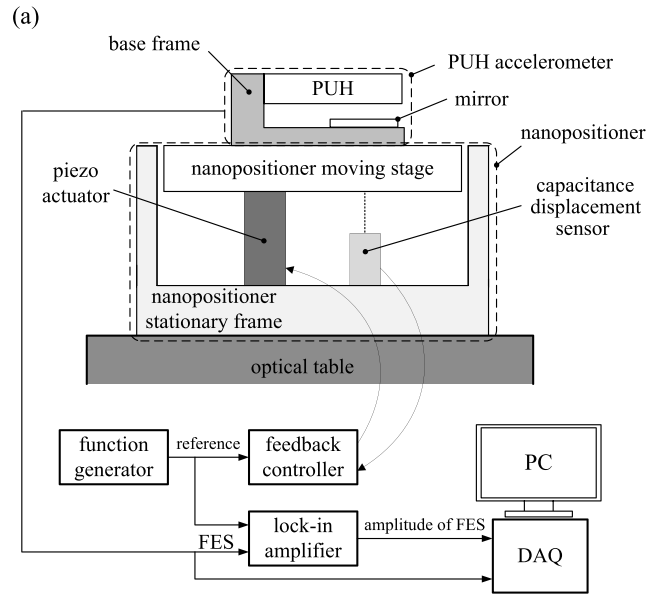
system is more compact and is easier to be implemented. The experiment in next section also shows that the considered mass-damper-spring system is properly damped for the application of accelerometers. The schematic illustration of the mechanical design of the proposed PUH accelerometer is shown in Fig. 6. A small mirror with a high quality reflecting surface is installed below the PUH, and a base frame separates the mirror and the PUH with a fixed gap. The structure loop has to be built solidly, or the internal vibration will induce a false signal. The material of the base frame is aluminum alloy and the total mass of all the mechanical parts is 0.04 kg.

IV. EXPERIMENT

To calibrate our DVD PUH-based accelerometer, a known excitation should be applied on it to record the output. A three-axis nanopositioner (NS4312-C, driven by NC3000 feedback controller, Nano Control Co., Ltd, Japan), on which our DVD PUH-based accelerometer is fastened, is employed to generate persistent excitation. A capacitance displacement sensor with 2 nm resolution is embedded on the z -axis; therefore, the acceleration of the nanopositioner can be known precisely. Without and with 0.1 kg payload, the resonant frequencies of the nanopositioner are 210 and 190 Hz, respectively [19]. A digital function generator (SFG-2010, Good Will Instrument Co., Ltd) decides the motion patent of the nanopositioner while a lock-in amplifier (SR830, Stanford Research Systems, Inc.) reveals the spectrum information of the accelerometer. To isolate the outside vibration, the accelerometer and the nanopositioner are installed on an optical table. A data acquisition card (DAQ, PCI-6036E, National Instruments) controls the focusing VCM of the accelerometer and records output signals. Fig. 7 shows the following experiments executed on the aforementioned set-up.

A. S-Curve

Because it is almost impossible to perfectly install the mirror at the middle of the linear region of the S-curve, the first experiment is rescanning the S-curve, and the result is shown in Fig. 8.



(b)

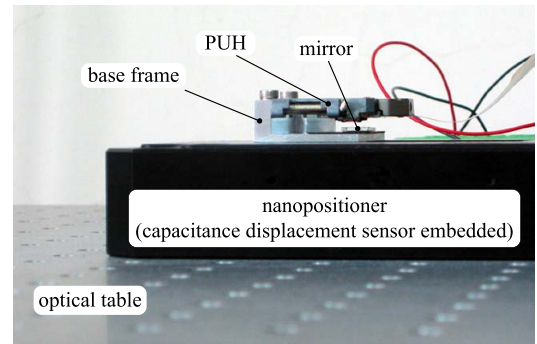


Fig. 7. (a) Schematic diagram and (b) photograph of the experimental set-up.

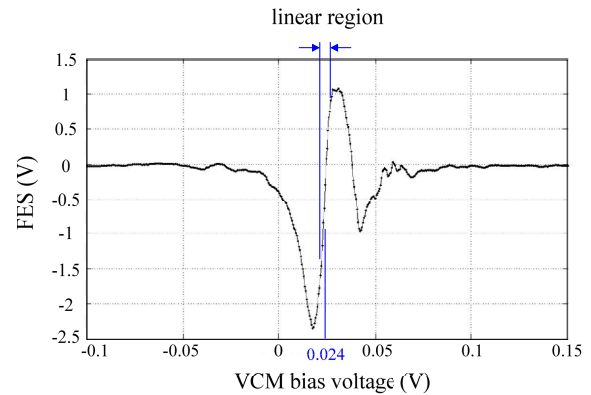


Fig. 8. Experimentally measured S-curve of the used DVD PUH.

Referring to Fig. 8 and applying a bias voltage of 0.024 V to the focusing VCM can move the objective lens to its best working point. The following experiments are conducted under this condition.

B. Dynamics

Now we inspect the dynamics of the mass-damper-spring system of our DVD PUH-based accelerometer. In this

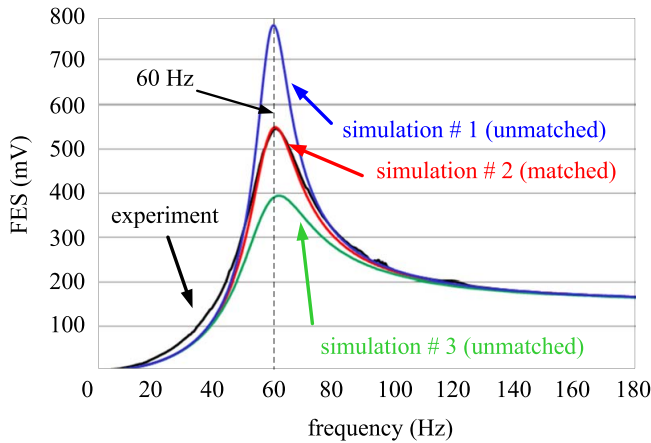


Fig. 9. Spectrum of the mass-damper-spring system of the PUH: experiment and simulation data.

experiment, the nanopositioner provides sinusoidal vibration to the accelerometer with controlled amplitude of constant $0.2 \mu\text{m}$ from 0.5 to 180 Hz, which is within the bandwidth of the nanopositioner [19]. The output is the FES of the accelerometer, which represents the relative displacement between the objective lens and the base. The measured spectrum is plotted in Fig. 9.

Moreover, from Fig. 1, an approximated model of the PUH mass-damper-spring system is represented as

$$m\ddot{q} + c\dot{q} + k(d - d_0) = 0 \quad (2)$$

where m is the seismic mass (i.e., objective lens), k is the spring (i.e., suspending metal wires), x is a sinusoidal function with constant amplitude and increasing frequency (i.e., chirp-like), d is the distance from the sensor to the seismic mass, $q = x + d$ is the position of the seismic mass in the inertial coordinate, and d_0 is the distance from the sensor to the seismic mass when the spring is at natural length. Let $v = d - d_0$, then (2) can be rewritten as

$$m(\ddot{x} + \ddot{v}) + c\dot{v} + kv = 0. \quad (3)$$

According to Laplace transfer function, (3) can be expressed as

$$\frac{V}{X} = \frac{-ms^2}{ms^2 + cs + k} \quad (4)$$

let $s = j\omega$, we have

$$\left| \frac{V}{X} \right| = \frac{m\omega^2}{\left[(k - m\omega^2)^2 + (c\omega)^2 \right]^{1/2}}. \quad (5)$$

Since FES is proportional to v , so we let $\text{FES} = Kv$, where K can be determined by the obtained data in Fig. 10. According to the experimental result and curve fitting, we have K is 190 mV/m . Seismic mass, m , is $2.8 \times 10^{-4} \text{ kg}$ by weighting disassembled moving parts of VCM. Now we try to estimate the spring constant k by Hook's Law. Flipping PUH upside down, the moving stroke of the seismic mass is double deflection caused by gravity. The moving stroke, $144 \mu\text{m}$, is measured by a laser displacement sensor (LK-H020, Keyence). Then, k can be calculated as 38 N/m by Hook's Law. From the

TABLE III
PARAMETERS OF SIMULATION

Parameter	simulation # 1 (unmatched)	simulation # 2 (matched)	simulation # 3 (unmatched)
K (mV/m)	190		
m (kg)	2.8×10^{-4}		
c (Ns/m)	0.02	0.0285	0.04
k (N/m)	38		

obtained data in Fig. 9, the resonant frequency is 60 Hz, which is 3.4% higher than the typical value of the specification, and the peak FES value at the resonant frequency is 546 mV. The shape of the spectrum also shows that it is not a low damping system, the damped natural frequency ω_n is 363.5 rad/s. So far, K , m , and k are fixed. The final parameter c can be determined by trial and error.

Scanning c value from 0.02 to 0.04 Ns/m, we found that the simulation and experiment curves are most fitted when $c = 0.0285 \text{ Ns/m}$. The identified parameters are listed in Table III and the corresponding simulation results are plotted in Fig. 9. The slight difference between experiment and simulation #2 is caused from the lumped linear model in (2). The order of the actual model would be higher than two because of the complex bending motion of the four parallel suspending wires.

C. Sensitivity

An accelerometer must work with frequency much far lower than its resonant frequency. According to the result of the previous experiment, we chose 10 Hz to investigate the low-frequency response of the proposed accelerometer. The nanopositioner shakes the accelerometer sinusoidally in vertical (focusing) direction at 10 Hz with the amplitude changing from 0 to $7 \mu\text{m}$. The acceleration that the nanopositioner gives to the accelerometer can be derived. Fig. 10 illustrates the response of the accelerometer. This result demonstrates that our accelerometer has excellent linearity 99.93% and ultrahigh sensitivity 114 V/g , which implies the capability to detect slight vibrations. The root mean square value of the background noise of FES is 1.8 mV , which is equivalent to 0.016 mg , i.e. the resolution of the proposed accelerometer. The noise may come from fluctuation of the laser source and the slight vibration of the seismic mass in horizontal (tracking) direction.

D. Operating Frequency

To find the operating frequency, the following experiment was implemented. The nanopositioner generated sinusoidal vibration from 0.5 to 30 Hz with a fixed $1 \mu\text{m}$ amplitude. The output voltage (FES) of the accelerometer can be converted into the corresponding acceleration using the sensitivity value obtained by the low-frequency response. Fig. 11 illustrates the experimental result. We can see that below 20 Hz, the operating frequency, the acceleration information produced by

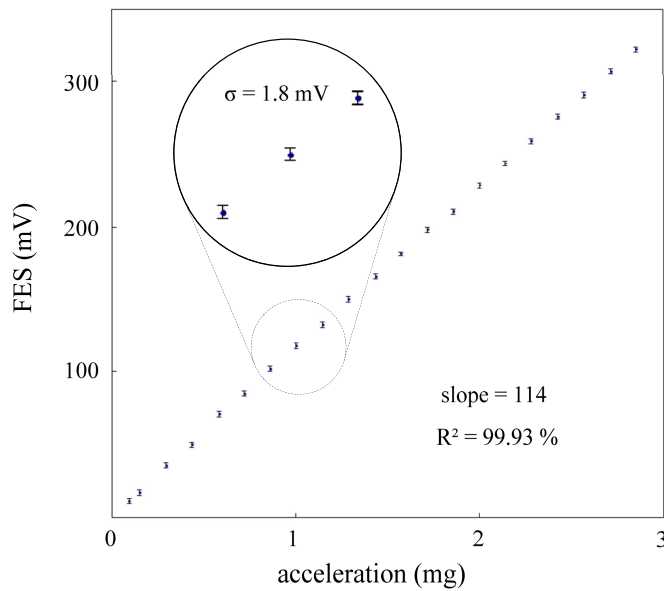


Fig. 10. Response of the proposed accelerometer at 10 Hz.

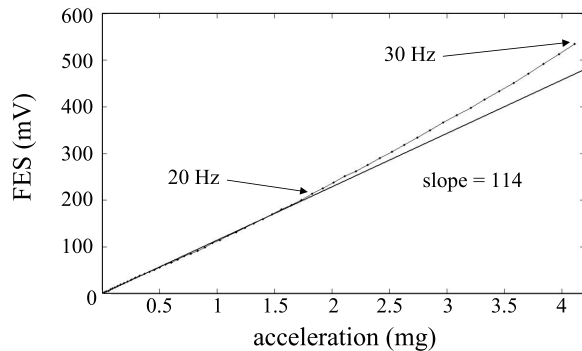


Fig. 11. Response of the proposed accelerometer from 0.5 to 30 Hz.

the PUH accelerometer has good agreement with the actual acceleration.

V. CONCLUSION

This paper proposes a method to transform a DVD PUH into an accelerometer. The suspending wires and objective lens, which are inside the DVD PUH itself function as a spring and a seismic mass, respectively. DVD's astigmatic mechanism functions as a displacement sensor to measure the vibration of the seismic mass, hence the acceleration is derived. This accelerometer has light weight of 0.04 kg, excellent linearity of 99.93%, ultrahigh sensitivity of 114 V/g, fine resolution of 0.016 mg, and an operating frequency below 20 Hz. This accelerometer is especially effective for low frequency and low magnitude applications, such as performance evaluation of vibration isolators. The resonant frequency and the acceleration magnitude of a typical passive optical table are <3 Hz and <3 mg, respectively. The other possible application is measuring non-sensible earthquakes. The frequency and acceleration magnitude of earthquakes at Mercalli intensity [20] scale 1 are 7–12 Hz and <1.7 mg, respectively.

In the future work, the seismic mass of PUH not only has focusing, but also has tracking degree-of-freedom. It is

possible to measure acceleration along two directions simultaneously if crosstalk effect is negligible. Furthermore, we will apply the proposed accelerometer to inspect the vibration level of floors in a laboratory or a factory. Furthermore, the proposed design of accelerometer using DVD PUH is very cost-effective so its commercial practicability is extended. This technology has been adopted to several vibration-sensitive instruments, such as stylus profilometers and AFMs. On the base of this paper, the next step is to develop an active vibration isolator.

REFERENCES

- [1] M. Serridge and T. R. Licht, *Piezoelectric Accelerometers and Vibration Preamplifiers*, Naerum, Denmark: Brüel & Kjær, 1987.
- [2] H. Xie and G. K. Fedder, "A CMOS z-axis capacitive accelerometer with comb-finger sensing," in *Proc. 13th Annu. Int. Conf. Micro Electro Mech. Syst.*, 2000, pp. 496–501.
- [3] J. G. T. Ribeiro, J. T. P. de Castro, and J. L. F. Freire, "Using the FFT-DDI method to measure displacements with piezoelectric, resistive and ICP accelerometers," in *Proc. Conf. Exposit. Struct. Dyn.*, 2003, pp. 1–7.
- [4] R. de Reus, J. O. Gullov, and P. R. Scheeper, "Fabrication and characterization of a piezoelectric accelerometer," *J. Micromech. Microeng.*, vol. 9, pp. 123–126, Nov. 1998.
- [5] P. Scheeper, J. O. Gullov, and L. M. Kofoed, "A piezoelectric tri-axial accelerometer," *J. Micromech. Microeng.*, vol. 6, pp. 131–133, Dec. 1995.
- [6] A. Partridge, J. K. Reynolds, B. W. Chui, E. M. Chow, A. M. Fitzgerald, L. Zhang, N. I. Maluf, and T. W. Kenny, "A high-performance planar piezoresistive accelerometer," *J. Microelectromech. Syst.*, vol. 9, no. 1, pp. 58–66, Mar. 2000.
- [7] H. Chen, M. Bao, H. Zhu, and S. Shen, "A piezoresistive accelerometer with a novel vertical beam structure," *Sens. Actuators A, Phys.*, vol. 63, no. 1, pp. 19–25, 1997.
- [8] E. A. Sani, R. S. Huang, and C. Y. Kwok, "A novel electromagnetic accelerometer," *IEEE Electron Device Lett.*, vol. 15, no. 8, pp. 272–273, Aug. 1994.
- [9] J. Kalenik and R. Pajgk, "A cantilever optical-fiber accelerometer," *Sens. Actuators A, Phys.*, vol. 68, nos. 1–3, pp. 350–355, 1998.
- [10] E. T. Hwu, S. K. Hung, C. W. Yang, I. S. Hwang, and K. Y. Huang, "Simultaneous detection of translational and angular displacements of micromachined elements," *Appl. Phys. Lett.*, vol. 91, no. 22, pp. 221908–221011, 2007.
- [11] K. C. Fan, C. L. Chu, and J. I. Mou, "Development of a low-cost autofocusing probe for profile measurement," *Meas. Sci. Technol.*, vol. 12, no. 12, pp. 2137–2146, 2001.
- [12] E. T. Hwu, S. K. Hung, C. W. Yang, K. Y. Huang, and I. S. Hwang, "Real-time detection of linear and angular displacements with a modified DVD optical head," *Nanotechnology*, vol. 19, no. 11, pp. 115501–115507, 2008.
- [13] C. L. Chu and C. H. Lin, "Development of an optical accelerometer with a DVD pick-up head," *Meas. Sci. Technol.*, vol. 16, no. 12, pp. 2498–2502, 2005.
- [14] C. L. Chu, C. H. Lin, and K. C. Fan, "Development of a two-dimensional optical accelerometer using a DVD pick-up head," *Proc. SPIE*, vol. 6280, pp. 62801M-1–62801M-6, Oct. 2006.
- [15] C. L. Chu and H. W. Liao, "Development of a tri-axial optical accelerometer using two DVD pick-up heads," *Proc. SPIE*, vol. 7130, pp. 713034-1–713034-6, Dec. 2008.
- [16] C. L. Chu, C. H. Lin, and K. C. Fan, "Two-dimensional optical accelerometer based on commercial DVD pick-up head," *Meas. Sci. Technol.*, vol. 18, no. 1, pp. 265–274, 2007.
- [17] F. Quercioli, B. Tiribilli, and A. Bartoli, "Interferometry with optical pickups," *Opt. Lett.*, vol. 24, no. 10, pp. 670–672, 1999.
- [18] A. Bartoli, P. Poggi, F. Quercioli, and B. Tiribilli, "Fast one-dimensional profilometer with a compact disc pickup," *Appl. Opt.*, vol. 40, no. 7, pp. 1044–1048, 2001.
- [19] (2007). Nano Control Co., Ltd. *Nano Servo Stage (Piezopositioner)*, Tokyo, Japan [Online]. Available: http://www.nanocontrol.co.jp/english/product/nanoservo/nsv_ns4312.html
- [20] U.S. Geological Survey. *ShakeMap Scientific Background*, Reston, VA, USA [Online]. Available: <http://earthquake.usgs.gov/earthquakes/shakemap/background.php>



Shao-Kang Hung (M'07) received the B.S. and M.S. degrees in mechanical engineering and the Ph.D. degree in electrical engineering from National Taiwan University, Taipei, Taiwan, in 1998, 2000, and 2007, respectively.

He has been with the Nanoscience Laboratory, Institute of Physics, Academia Sinica, Taipei, since 2000, where he involved in nanopositioning and scanning probe microscopy. Since 2008, he has been a member of the faculty with National Chiao-Tung University, Hsinchu, Taiwan, where he is currently an Assistant Professor with the Department of Mechanical Engineering. His current research interests include opto-mechatronic systems, nanometer-scale instrumentation, and precision motion control.



Ming-Li Chiang received the Ph.D. degree in electrical engineering from National Taiwan University, Taipei, Taiwan, in 2010.

He is currently a Post-Doctoral Fellow with the Department of Electrical Engineering, National Taiwan University. His current research interests include switched systems, adaptive control, robust control, and nonlinear control systems.



Chiao-Hua Cheng received the B.S. and M.S. degrees in mechanical engineering from National Chiao-Tung University, Hsinchu, Taiwan, in 2009 and 2011, respectively, where he is currently pursuing the Ph.D. degree in mechanical engineering.

His current research interests include inertia motor, atomic force microscopy, and microprototyping.



Jih-Wei Chieh received the B.S. degree in transportation and management and the M.S. degree in mechanical engineering from National Chiao-Tung University, Hsinchu, Taiwan, in 2008 and 2010, respectively.

He has been with WECON, Hsinchu, since 2011.